OPEN ACCESS

Life Science Leaflets Vol. 178, 2025 pp.13–35 .....*e-ISSN: 2277-4297 (online), ISSN:2277-4297(Print)*

EVALUATION OF LAND USE LAND COVER (LULC) CHANGES IN THE DIU ISLAND OF THE SAURASHTRA REGION FOR SUSTAINABLE RESTORATION OF HISTORIC LANDMARKS

KAVYA P. TANNA[2] AND REENA P. DAVE[1]*

Department of Biology,
Shree M. & N. Virani Science College (Autonomous), Rajkot, Gujarat, India.
Corresponding author's email: reenadave23@gmail.com

(Received on: 2nd January 2025; Revised on: 15th January 2025;
Accepted on: 20th January 2025; Published on: 1st February 2025)

ABSTRACT:

Diu city of Gujarat, India is well known city for it traditional heritage sites of Portuguese and Indian culture. It has various natural and man-made heritage sites such as beaches, coastal flora, fauna, rocky creeks, stone quarries, Fort, churches, museum, temples, mosques, markets squares, traditional houses, cross, pillars, and statues which attracts tourists from different places of the world. In order to know the changes in land use and land cover in this city due to urbanization and its impact on maintenance of heritage sites during the past 30 years present studies were carried out. The study primarily focused on the land use and land cover deviations using Maximum Likelihood (MXL) Classification algorithm to classify the Landsat 5 and 8 imageries of the year 1991, 2001, 2011 and 2021 in QGIS software. The changes in various parameters like residential and commercial constructions, wild and anthropogenic vegetation cover, water bodies and open land area in Diu city were observed in LULC maps. Overall accuracy of the data was determined with the help of ESRI ArcGIS® through Kappa statistics. The post–classification comparison method helped in identification of changes occurred in the Diu city during last 30 years due to urbanization. From present studies it was observed that there was gradual decrease in open land in the city from year 1991 to 2021 which is utilized either for built up of hotels/resorts, tourism sites, commercial complexes, development of anthropogenic vegetation, or lakes in the city for socioeconomic development and urbanization.

KEY WORDS: *Tourism, LULC, Waterbodies, anthropogenic vegetation, Diu.*

INTRODUCTION:

A dynamic study of land use and land cover (LULC) provides a thorough understanding of the connections and correlations between fluctuations in the Earth's surface and human activity (Prakasam, 2010; Mmbaga et al., 2017). To take into account a variety of biophysical, ecological, social, and climatic implications and to ensure the sustainable management of natural resources, it is critically important to analyze LULC changes (Turner, 2002; Foley et al., 2005; Drummond and Loveland, 2010; Ayele et al., 2018). Due to an increase in anthropogenic activities and their interactions with climatic change in recent years, LULC changes have happened quickly (Deng et al., 2013; M'mboroki et al., 2018; Gogoi et al., 2019). They are a significant source of worry for regional and global environmental changes (Yuan et al., 2013), which have a significant impact on biodiversity, ecological balances, and carbon (C) cycling (Haines-Young, 2009; Khoi and Murayama, 2010; Behera et al., 2012; Liping et al., 2018; and Sleeter et al., 2018). Forest losses and agricultural gains have typified the global track of LULC changes over the last 300 years (Houghton, 2003; Yin et al., 2011). (Pielke et al. 2011) claimed that agricultural growth and intensification were the main forces behind LULC shifts worldwide. To comprehend and evaluate the magnitude and implications at a local, regional, and global scale, a systematic, accurate, and current assessment of LULC changes is necessary (Potapov et al., 2008; Kim, 2016; Liping et al., 2018). The historic monument city of Diu is located at the eastern end of western India near the seashore of the Arabian Sea. It is listed as the union territory along with Daman, Dadra, and Nagar Haveli of India. Even today, it shows the exclusive combination of traditional Portuguese and Indian culture. It has various natural and man-made heritage sites which attract tourists from different places of the world. The natural heritages include beaches, coastal flora, fauna, rocky creeks, and stone quarries. The man-made heritages include Fort, churches, museum, temples, mosques, market squares, traditional houses, cross, pillars, and statue. It stands for live traditions and testimony that are being practiced and transmitted continuously from one generation to another. These traditions are seen in myriads and rituals followed during festivals, dances, ancient arts, and handicrafts. There are dance forms (Garba, Siddi dhamal, and Portuguese) and Fairs observed during festivals such as Christmas, Nariyal Purnima, Madhi, Navratri, and Vatva. The ancient art and handicraft work seen in this city is silk weaving, wall paintings, dyeing, and block printing (Harsimran et. al. 2015). Diu is famous for impressive heritage memorials, silent beaches, ancient Portuguese architecture, and exotic liquor. It has a unique built and cultural heritage that has attracted millions of tourists for many years and is a prime source of economy for the local community living there. However, there has been a 60% fall in the number of foreign tourists since 2001 over the previous years. Even, there is a shift in tourist profile with an increase in Asian and African tourists and a decrease in Western and Northern American tourists since the year 1999 to 2010. This is due to the need for restoration and maintenance of urban spaces, coastal natural habitats, heritage sculptures, and unique environments for tourists to stay longer in the city.

The historic core area of the city and heritage places are continuously degrading due to tremendous development pressure, improper management of traditional practices, and lack of awareness among tourists as well as the local community. It has a major challenge of building sustainable development plans that integrates and maintains the beauty of cultural heritage sites. It is necessary to link city development, local community development, and cultural heritage maintenance plans. Hence, the present study was carried out to give information on the significant variation in land use and land cover of Diu City in the past 30 years (from 1991 to 2021) which will help to develop sustainable development plans for maintenance of natural and man-made heritage sites.

MATERIALS AND METHOD:

Study Area:

Diu is a small island off the coast of Gujarat, near the Port of Veraval, with a coastal length of 21 kilometres and a distance of 768 kilometres from Daman, the newly formed Union Territory of Daman and Diu's capital. Diu is bordered on the north by Gujarat's Gir-Somnath and Amreli districts, and on three sides by the Arabian Sea which makes it a fishing town. It is connected to the mainland by two bridges. The Diu district is located between the meridians 71°-00'-24" and 70°-52'-26" of longitude east of Greenwich, and between the parallels 20°-44'-34" and 20°-42'-00" of latitude north. It is 4.6 kilometres in length from north to south and 13.8 kilometres in width from east to west. The island is 38.8 square kilometres (15.0 square miles) in size and is at sea level. With an average annual rainfall of 560 mm (22 in) throughout the year but 25 mm (1.0 in) falling between June and September, Diu has a hot, semi-arid climate (Köppen BSh).According to reports from April 2018, the Diu Smart Metropolis has already become India's first city to run entirely on renewable energy throughout the day. The Hoka trees (a species of palm tree found nowhere else in India), which grow edible fruit, are another distinctive feature of Diu.

Methodology:

In present studies, clear satellite images downloaded from USGS (United States geological survey) Earth Explorer were combined and demographic data was generated to interpret the land use and land cover changes. Each satellite image was classified using the Maximum Likelihood Classifier (MXL) approach. The generated LULC maps were then compared using a change detection matrix utilizing a pixel-by-pixel technique. The methodology which has been carried out in this research is as follows:

Data Collection and Pre-processing:

The alterations in the LULC were assessed using satellite pictures from 1991 to 2021. The satellite image of the years 1991, 2001, 2011 & 2021 were downloaded from the United States Geological Survey's Earth Explorer web archive (freely downloadable worldwide). The scene of the satellite image of the year 1991 was covered by the Landsat 5 TM having path 153 and row 5. Similarly, one scene of the satellite image of the year 2001 and 2011 were covered by using the Landsat 5 TM

having path 153 and row 5. The scene of the satellite image of the year 2021 was covered by the Landsat 8 OLI–Thermal Infrared Sensor (TIRS) having Path 143 and row 51. The Landsat 5 TM contains four spectral bands (4–7) with a spatial resolution of 30 m, while Landsat 8 OLI contains nine spectral bands (2–7) with a spatial resolution of 30 m (Table:1). The LULC map was made using these satellite images in QGIS software version 3.20.1. satellite images downloaded were saved as a Geo Tiff file in the form of a greyscale image of the research region, each image band shows intensity values for a certain wavelength. Images with cloud cover and unwanted shade cause hindrances during the categorization of classes and decrease the accuracy. hence, only high-quality, cloud-free scenes were considered in the study.

Supervised Classification:

With the help of Google Maps, a shapefile of Diu City was created in Google Earth Pro (Fig:1). Satellite images from the USGS Earth Explorer website and the Landsat satellite covering the study area were obtained. In QGIS Desktop 3.20.1, the pictures were further processed by performing supervised land use and land cover classification. The city was categorized into four different classes: 1) wild or anthropogenic vegetation, 2) built-up (concrete constructions), 3) water bodies, and 4) open land (Table:2). Land cover types were classified using multi-temporal Landsat images of the research area (Vivekananda et. al. 2021). The classified images of the years 1991, 2001, 2011, and 2021 were compared with each other to observe the variation in the LULC pattern.

Selection of Training Data Samples:

This method allowed the research area's distinct traits to be identified. A variety of band combinations were employed to determine a class's color tone. For vegetation, forest, crops, and wetlands investigation, the band combination 5–4–3 was employed. The built-up land was analyzed using the band combination 7–6–4 (Table: 1). The tone of the pixel color was used to train data sets. Drawing polygons and placing them in an AOI (Area of Interest) layer were used to generate training sites in the imagery. 15 polygons were brought in and placed in the signature editor to train each class. These 15 polygons were combined and given a unique class name. Finally, in the supervised image classification procedure, the trained data sets were utilized.

Classification Accuracy Assessment using the Confusion matrix:

The accuracy of classified images was determined with the help of ESRI ArcGIS software using the method determined by Foody, 2002. In ArcGIS, a shapefile named ‘Point’ was created in the layers panel and projected to the Geographic (Lat/Lon) WGS 1984 datum. Randomly, 25 to 30 points (each with specific color and pixel value) were created on the classified images of each city and each year. The classes in the classified image were used as reference points. Following the detection of randomly generated spots, the user manually assigned the correct class. The shapefile was then converted into a kml file and opened in Google Earth Pro for checking the accuracy. The error matrix determines the percent accuracy of the classification.

When a categorization technique allocates pixels to a certain class that they do not belong to, errors of commission arise. In column cells above and below the major diagonal of the class, it was possible to count the number of pixels that were mistakenly allocated to that class. The number of commission errors was also specified by the Producer's accuracy. Pixels from one class were included in pixels from other classes, resulting in omission errors for each class. The number of missed pixels was found in the row cells to the left and right of the major diagonal in the confusion matrix. Omission errors occurred for each class as a result of pixels from one class being combined with pixels from another. The equations used for accuracy assessment are as mentioned below**:**

User's Accuracy: $\frac{\text{Number of correctly classified pixels in each category}}{\text{Total number of classified pixels in that category (the row total)}} \times 100$

Producer's Accuracy: $\frac{\text{Number of correctly classified pixels in each category}}{\text{Total number of reference pixels in that category (the column total)}} \times 100$

Kappa Coefficient: $\frac{(\text{TS} \times \text{TCS}) - \sum (\text{Column Total} \times \text{Row Total})}{\text{TS2} - \sum (\text{Column Total} - \text{Row Total})} \times 100$

Where,

TS = Total Samples

TCS = Total Correctly Classified Samples

Change Detection through Post-classification comparison technique:

Remote-sensing and GIS-based change detection are widely used to determine LULC changes due to their spatiotemporal high resolution. In present studies, the maximum likelihood supervised classification-based post-classification comparison technique (Muttitanon & Tripathi, 2005; Torahi & Rai, 2011) was used for detecting LULC changes that occurred in Diu City due to urbanization. The post-classification comparison has classified the images and compared the respective classes with each other to determine the areas where changes have occurred based on Maximum Likelihood Classifier (MXL) algorithm (Sun & Wang, 2009; Team, 2014) to verify the land use changes. The two registered and independently classified images were used to calculate the land use changes and the degree of accuracy was determined through the thematic map of image classification. The magnitude of change in each class was determined by using the following formula:

$$\mathbf{Ci = Li - Bi}$$

Where,

i = Number of classes in an image,

Ci = Magnitude of change in class "i.",

Li = Base image (1991)

Bi = Latest image (2021)

The percentage change (C %) in each land-use class was determined by using following formula

$$Pi = (Li - Bi / Bi) x 100$$

Where: Pi = Percentage of change in class "i"

Statistical analysis:

All the measured parameters were subjected to Principal component analysis using clusters: a web tool (https://biit.cs.ut.ee/clustvis/) to determine the significant relationship of one component with another.

RESULTS AND DISCUSSION:

In present studies, satellite pictures from the USGS Earth Explorer website and the Landsat satellite covering the study area of the shapefile were obtained (Fig:1) because Earth Science Data Systems NASA releases a PALSAR radiometrically terrain corrected (RTC) digital elevation model (DEM) with a 12.5-m spatial resolution to acquire the topography characteristics (Logan et al. 2014). In the present study, Diu City was categorized into four different classes (wild & anthropogenic vegetation, built-up, waterbodies, and open land) in terms of supervised land use land cover classification scheme using the Maximum likelihood classifier algorithm. As Maximal Likelihood is a Bayes Theorem-based supervised classification method in which the classifier computes the probability that a pixel belongs to a class. To create a LULC map of each band-set image, the classifier is trained one by one for each image in the prepared dataset (Mishra and Jabin; 2020; Gupta and Sharma; 2020). Similarly, Anil et al., 2011; Bayarsaikan et al., 2009; Brahabhatt et al., 2000; Ratnaparkhi et al., 2016; Iqbal & Iqbal, 2018) have also employed the Maximum likelihood classifier algorithm to classify satellite imagery in their study areas.

Spatio-temporal changes in the Land use due to urbanization in Diu city:

From the supervised classification of land use and land cover analysis, it was observed that the wild & anthropogenic vegetation cover in Diu City during the year 1991 was 0.29 km2 which increased during the years 2001 and 2011 to 0.51 km2 and 0.60 respectively. However, a decrease in vegetation cover of Diu City was observed due to anthropogenic activities during the year 2021 which is 0.43 km2. The built-up area in Diu City during the year 1991 was 0.87 km2 which increased during the year 2001 to 0.97 km2 and slightly increased again to 1.15 km2 in the year 2011. However, build-up increased exponentially during the year 2021 to 1.42 km2. The area coverage of water bodies in Diu City during the year 1991 was 0.24 km2 which gradually increased during the years 2001 to 2021 from 0.37 km2 to 0.39 km2 respectively, due to the development of anthropogenic lakes. The open land during the year 1991 was 1.34 km2 which decreased gradually to 0.90 km2, 0.65 km2, and 0.50 km2 during the years 2001, 2011, and 2021 respectively due to an increase in build-up areas and anthropogenic water bodies (Table: 3, Fig:2). The Principal component analysis grouped the data into four groups based on LULC supervised classification. Group A included the year 1991 which had low vegetation cover, built and water bodies, and high

open land. Group B included the year 2001 which shows the utilization of open land in the development of anthropogenic waterbodies and vegetation cover. Group C included the year 2011 which shows the utilization of open land in built-up and anthropogenic vegetation cover. Group D included the year 2021 which shows the utilization of open land in built-up and anthropogenic waterbodies development (Fig: 3 & 4).

Accuracy Assessment of LULC maps using Confusion matrix:

Accuracy assessment of LULC images for the years 1991, 2001, 2011, and 2021 were carried out using Arc GIS software. For the year 1991, it was observed that overall accuracy was 95.83% and Kappa's Coefficient was 94.44%. The user's accuracy for all the classes (wild or anthropogenic vegetation, built-up and open land) was 100% except for the waterbody class, which had 83.33% accuracy. The producer's accuracy for all the classes (wild or anthropogenic vegetation, agriculture land, built-up, water bodies, and open land) was above 80%. For the year 2001, it was observed that overall accuracy was 95.83% and Kappa's Coefficient was 94.44%. The user's accuracy for the classes (wild & anthropogenic vegetation, built-up, waterbody, and open land) was equal to or above 80%. The producer's accuracy for the classes (wild & anthropogenic vegetation, built-up, waterbody, and open land) was equal to or above 80%. For the year 2011, it was observed that overall accuracy was 95.83% and Kappa's coefficient was 94.44%. The user's accuracy for all the classes was equal to or above 80%. The producer's accuracy for all the classes was equal to or above 80%. For the year 2021, overall accuracy was 100% and Kappa's coefficient was 100%. The user's accuracy for all the classes was 100%. The producer's accuracy for all the classes was 100% (Table: 4). These Kappa values for the four classification findings are satisfactory for the research region since they meet Anderson's (Anderson, J.R.; 1976) classification scheme's minimal accuracy requirement. These findings provide a solid foundation for further research on LULC changes. To determine the correctness of the information gathered for the images, a classification assessment was performed. It is critical to establish good accuracy on individual classed images to deploy fruitful change detection techniques on the images and obtain correct findings. The accuracy of the classification is determined by comparing reference data to the classification results using error matrices (Mishra and Jabin; 2020).

Change detection of Diu city from year 1991 to 2021 using post-classification:

comparison technique:

From the post-classification comparison analysis, change detection was observed in Diu City from the year 1991 to 2021. The wild and anthropogenic vegetation increased from 0.29 km2 in the year 1991 to 0.43 km2 in the year 2021 due to an increase in vegetation nearby tourism sites, hotels, and resorts for beautification purposes. There was a remarkable increase in build-up areas from 0.87 km2 in 1991 to 1.42 km2 in 2021 due to the growth in commercial complexes, residential houses, tourist settlements, spas, resorts, and hotels. The area covered by water bodies increased from 0.24 km2 in 1991 to 0.39 km2 in 2021 due to the development of swimming pools in hotels/ resorts as well as the

build-up of anthropogenic lakes at tourism sites. The area covered by open land decreased from 1.34 km2 in 1991 to 0.54 km2 in 2021 because of a remarkable exponential increase in build-up areas on the open land due to the development of resorts, hotels, spas, commercial complexes, and residential areas in Diu city (Table: 5, Fig: 5). In present studies, change detection of LULC maps was done because post-classification comparisons are effective tools which determine the type and frequency of changes that occur in a particular region over time. The images are analysed pixel by pixel and then a cross-tabulation is created to determine the alteration of pixels from one land cover class to another (Misra & Jabin 2020).

CONCLUSIONS:

In present studies, LULC maps were generated by using remote sensing and GIS techniques to study the land use changes in the city of Diu due to urbanization in the last 30 years. From LULC analysis it was observed that there was a remarkable change in the land use and land cover in Diu City from the year 1991 to 2021 due to urbanization. There was an increase in anthropogenic vegetation in the city due to an increase in vegetation nearby tourist sites, hotels, and resorts for decoration purposes. There was an increase in built-up areas in the city due to the development of resorts, hotels, spas, commercial complexes, and residential areas. There was an increase in anthropogenic water bodies in the city due to the development of anthropogenic lakes at tourism sites and swimming pools in hotels and resorts. There was an exponential decrease in open land from the year 2011 to 2021 due to the construction of buildings, anthropogenic lakes, and human-cultivated vegetation in residential and industrial areas. The overall accuracy of data was confirmed by using a confusion matrix and kappa statistics. The post-classification analysis helped in the identification of changes that occurred during the last 30 years due to the development of industries and socioeconomic development. The sustainable increase in anthropogenic vegetation and water bodies in the city during the last 30 years supports ecosystem services and the beautification of the region. There was a remarkable increase in built up of hotels, resorts, spas, and commercial complexes in the city which increases the attraction of tourists.

Ethical Approval: Ethical approval is not required to publish the present research data in the journal

Consent to Participate: Authors provide consent to participate in the publication process of the present research data in the journal

Consent to Publish: Authors provide consent to publish the present research data in the journal

Authors Contributions:

1) Ms. Kavya Tanna: Data generation, Data analysis, write up of manuscript
2) Dr. Reena P. Dave: Data analysis, data interpretation, write up of manuscript

Funding: No funding was available for this research work

Competing Interests: Authors declare that there is no conflict of interest regarding publication of the research article in the Journal

Availability of data and materials: Data is included in the manuscript in the form of figures and Tables

ACKNOWLEDGMENTS:

Authors are thankful, Shree M. & N. Virani Science College (Autonomous) and SRTD-RTCG-MISA, Space Application centre (ISRO). Ahmedabad, Gujarat for providing the training and working facility to carry out this research work

REFRENCES:

1. Anderson, J. R. (1976). *A land use and land cover classification system for use with remote sensor data* (Vol. 964). US Government Printing Office, Washington, DC, USA.
2. Anil, N. C., Jai Sankar, G., Jagannadha Rao, M., Prasad, I. V. R. K. V., & Sailaja, U. (2011). Studies on land use/land cover and change detection from parts of South West Godavari District, A.P-using remote sensing and GIS techniques. Journal of Indian Geophysical Union, 15(4), 187–194.
3. Ayele, G. T., Tebeje, A. K., Demissie, S. S., Belete, M. A., Jemberrie, M. A., Teshome, W. M., Teshome D. T. Mengistu & Teshale, E. Z. (2018). Time series land cover mapping and change detection analysis using geographic information system and remote sensing, Northern Ethiopia. Air, Soil and Water Research, 11, 1178622117751603.
4. Bayarsaikan, U., Boldgiv, B., Kim, K., Park, K., & Lee, D. (2009). Change detection and classification of land cover at Hustai National Park in Mongolia. International Journal of Applied Earth Observation and Geoinformation, 11(4), 273–280.
5. Behera, M. D., Borate, S. N., Panda, S. N., Behera, P. R., & Roy, P. S. (2012). Modelling and analyzing the watershed dynamics using Cellular Automata (CA)–Markov model–A geo-information based approach. Journal of earth system science, 121, 1011-1024.
6. Brahabhatt, V. S., Dalwadi, G. B., Chnabra, S. B., Ray, S. S., & Dadhwal, V. K. (2000). land use/land cover changes mapping in Mahi canal command area, Gujarat, using multi-temporal satellite data. Journal of Indian Socity Remote Sensing, 28(4), 221–232.
7. Deng, X., Zhao, C., & Yan, H. (2013). Systematic modeling of impacts of land use and land cover changes on regional climate: a review. Advances in Meteorology, 2013, 1-11.
8. Drummond, M. A., & Loveland, T. R. (2010). Land-use pressure and a transition to forest-cover loss in the eastern United States. BioScience, 60(4), 286-298.
9. Foley, J. A., DeFries, R., Asner, G. P., Barford, C., Bonan, G., Carpenter, S. R., & Snyder, P. K. (2005). Global consequences of land use. science, 309(5734), 570-574.
10. Foody, G. M. (2002). Status of land cover classification accuracy assessment. Remote Sensing of Environment, 80 (1), 185–201.
11. Gogoi, P. P., Vinoj, V., Swain, D., Roberts, G., Dash, J., & Tripathy, S. (2019). Land use and land cover change effect on surface temperature over Eastern India. Scientific reports, 9(1), 8859.

12. Gupta, R., & Sharma, L. K. (2020). Efficacy of Spatial Land Change Modeler as a forecasting indicator for anthropogenic change dynamics over five decades: A case study of Shoolpaneshwar Wildlife Sanctuary, Gujarat, India. Ecological Indicators, 112, 106171.

13. Haines-Young, R. (2009). Land use and biodiversity relationships. Land use policy, 26, S178-S186.

14. Houghton, R. A. (2003). Revised estimates of the annual net flux of carbon to the atmosphere from changes in land use and land management 1850–2000. *Tellus B: Chemical and Physical Meteorology*, *55*(2), 378-390.

15. Iqbal, M. Z., & Iqbal, M. J. (2018). Land use detection using remote sensing and gis (A case study of Rawalpindi Division). *American Journal of Remote Sensing*, *6*(1), 39-51.

16. Kaur Harsimran, Ahuja Rita and Praharaj Sarbeswar (2015). Revitalization of the Historic Urban Quarters and Upgrading Tourism Economy in the Walled City of Diu, India (HISTORIC CITIES: TRANSFORMATION OF HISTORIC CITIES). Conference Paper · April 2015 DOI: 10.13140/RG.2.1.1821.4489

17. Khoi, D. D., & Murayama, Y. (2010). Forecasting areas vulnerable to forest conversion in the Tam Dao National Park Region, Vietnam. Remote sensing, 2(5), 1249-1272.

18. Kim, C., (2016). Land use classification and land use change analysis using satellite images in Lombok Island, Indonesia. For. Sci. Technol. 12 (4), 183–191.

19. Liping, C., Yujun, S., & Saeed, S. (2018). Monitoring and predicting land use and land cover changes using remote sensing and GIS techniques—A case study of a hilly area, Jiangle, China. PloS one, 13(7), e0200493 1-23.

20. Logan, T. A., Nicoll, J., Laurencelle, J., Hogenson, K., Gens, R., Buechler, B., Barton, B., Shreve, W., Stern, T., Drew, L. & Guritz, R. (2014). Radiometrically terrain corrected ALOS PALSAR Data available from the Alaska Satellite Facility. In *AGU Fall Meeting Abstracts* (Vol. 2014, pp. IN33B-3762).

21. M'mboroki, K. G., Wandiga, S., & Oriaso, S. O. (2018). Climate change impacts detection in dry forested ecosystem as indicated by vegetation cover change in—Laikipia, of Kenya. Environmental monitoring and assessment, 190, 1-19.

22. Mishra, S., & Jabin, S. (2020, October). Land Use Land Cover Change Detection using LANDSAT images: A Case Study. In 2020 IEEE 5th International Conference on Computing Communication and Automation (ICCCA) (pp. 730-735). IEEE.

23. Mmbaga, N. E., Munishi, L. K., & Treydte, A. C. (2017). How dynamics and drivers of land use/land cover change impact elephant conservation and agricultural livelihood development in Rombo, Tanzania. Journal of Land Use Science, 12(2-3), 168-181.

24. Muttitanon, W., & Tripathi, N. (2005). Land use/land cover changes in the coastal zone of Ban Don Bay, Thailand using Landsat 5TM data. International Journal of Remote Sensing, 26(11), 2311–2323.

25. Pielke Sr, R. A., Pitman, A., Niyogi, D., Mahmood, R., McAlpine, C., Hossain, F., Goldewijk KK, Nair U, Betts R, Fall S, Reichstein M. (2011). Land use/land cover changes and climate: modeling analysis and observational evidence. Wiley Interdisciplinary Reviews: Climate Change, 2(6), 828-850.

26. Potapov, P.V., Yaroshenko, A., Turubanova, S., Dubinin, M., Laestadius, L., Thies, C., Aksenov, D., Egorov, A., Yesipova, Y., Glushkov, I., et al., (2008). Mapping the world's intact forest landscapes by remote sensing. Ecol. Soc. 13 (2), 51.

27. Prakasam, C. (2010). Land use and land cover change detection through remote sensing approach: A case study of Kodaikanal taluk, Tamil nadu. International journal of Geomatics and Geosciences, 1(2), 150-158.

28. Ratnaparkhi, N. S., Ajay, D. N., & Bharti, G. (2016). Analysis of land use/land cover changes using remote sensing and GIS techniques in Parbhani City, Maharasthra, India. International Journal of Advanced Remote Sensing and GIS, 5(1), 1702–1708.

29. Sleeter, B. M., Liu, J., Daniel, C., Rayfield, B., Sherba, J., Hawbaker, T. J., Hawbaker, Z. Zhu, P. C. Selmants & T. R. Loveland (2018). Effects of contemporary land-use and land-cover change on the carbon balance of terrestrial ecosystems in the United States. *Environmental Research Letters*, *13*(4), 045006.

30. Sun, Z. M. A. R., & Wang, Y. (2009). Using Landsat data to determine land use changes in Datong basin, China. Environmental Geology, 57(8), 1825–1837.

31. Team, D. (2014). QGIS geographic information system. Open-Source Geospatial Foundation Project.

32. Torahi, A. A., & Rai, S. C. (2011). Land cover classification and forest change analysis, using satellite imagery-A case study in Dehdez area of Zagros Mountain in Iran. Journal of Geographic Information System, 3(1), 1–11.

33. Turner, B. L. (2002). Toward integrated land-change science: Advances in 1.5 decades of sustained international research on land-use and land-cover change. In *Challenges of a Changing Earth: Proceedings of the Global Change Open Science Conference, Amsterdam, The Netherlands, 10–13 July 2001* (pp. 21-26). Springer Berlin Heidelberg.

34. Vivekananda GN, Swathi R & Sujith AVLN (2021) Multi-temporal image analysis for LULC classification and change detection, European Journal of Remote Sensing, 54, 189-199.

35. Yin, J., Yin, Z., Zhong, H., Xu, S., Hu, X., Wang, J., & Wu, J. (2011). Monitoring urban expansion and land use/land cover changes of Shanghai metropolitan area during the transitional economy (1979–2009) in China. Environmental monitoring and assessment, 177, 609-621.

36. Yuan, Y., Zhao, T., Wang, W., Chen, S., & Wu, F. (2013). Projection of the spatially explicit land use/cover changes in China, 2010–2100. Advances in Meteorology, 2013, 1-9.

Table 1: Spectral characteristics of the Landsat data used for assessing the LULC changes in the study area

Satellite	Spatial Resolution	Spectral Bands	Wavelength	Data Source
Landsat 8 OLI/TIRS	30 m	Band 1 – Ultra Blue	0.43-0.45	www. usgs.gov.in
		Band 2 – Blue	0.45-0.51	
		Band 3 – Green	0.53-0.59	
		Band 4 – Red	0.64-0.67	
		Band 5 – Near Infrared	0.85-0.88	
		Band 6 – Shortwave (Infrared 1)	1.57-0.65	
		Band 7 – Shortwave (Infrared 2)	2.11-2.29	
		Band 8 – Panchromatic	0.50-0.68	
		Band 9 – Cirrus	1.36-1.38	
		Band 10 - Thermal Infrared (TIRS) 1	10.6-11.19	
		Band 11 - Thermal Infrared (TIRS) 2	11.50-12.51	
Landsat 5 TM	30 m	Band 1	0.45-0.52	WWW USGS.gov.in
		Band 2	0.52-0.60	
		Band 3	0.63-0.69	
		Band 4	0.76-0.90	
		Band 5	1.55-1.75	
		Band 6	10.40-12.50	
		Band 7	2.08-2.35	

Table 2: Details of Image Classification used in supervised classification scheme

Sr. No.	Class	Description
1	WILD & ANTHROPOGENIC VEGETATION	Land characterized by relatively sparse wild vegetation & vegetation surrounding hotel, guest house and resorts. Areas characterized by a high density of grasses, herbs, and crops, including parks and regularly tilled, planted croplands
2	BUILT-UP	Land covered by concrete, including low-, medium, and high-density road networks; residential, industrial, Resorts, Spa, Hotel, Guest House and commercial buildings; educational institutes; transportation; open-roof concrete structures; other human-made structures; and solid waste landfills
3	WATERBODY	Areas covered by water, including reservoirs, ponds, lakes, and streams and anthropogenic waterbodies.
4	OPEN LAND	Areas with or without sparse vegetation that are likely to change or be converted to other users in the future. This category includes land without crops, land with barren rock, and sand areas along rivers/stream beaches

Table 3: Supervised classification of the Diu city to study spatio-temporal changes in land use from the year 1991 to 2021

Class	PixelSum	Percentage %	Area [metre^2]	Area per sq. km
Year:1991				
WILD VEGETATION	3752	5.15	3376800	3.38
ANTHROPOGENIC VEGETATION	7944	10.90	7149600	7.15
BUILT-UP	5777	7.93	5199300	5.20
WATERBODY	6338	8.70	5704200	5.70
OPEN LAND	17997	24.70	16197300	16.20
Year:2001				
WILD VEGETATION	4492	6.16	4042800	4.04
ANTHROPOGENIC VEGETATION	5633	7.73	5069700	5.07
BUILT-UP	3901	5.35	3510900	3.51
WATERBODY	6388	8.77	5749200	5.75
OPEN LAND	21394	29.36	19254600	19.25
Year: 2011				
WILD VEGETATION	5934	8.14	5340600	5.34
ANTHROPOGENIC VEGETATION	7668	10.52	6901200	6.90
BUILT-UP	4190	5.75	3771000	3.77
WATERBODY	7272	9.98	6544800	6.54
OPEN LAND	16744	22.98	15069600	15.07
Year: 2021				
WILD VEGETATION	958	1.31	862200	0.86
ANTHROPOGENIC VEGETATION	7275	9.98	6547500	6.55

BUILT-UP	10849	14.89	9764100	9.76
WATERBODY	13043	17.90	11738700	11.74
OPEN LAND	9683	13.29	8714700	8.71

Table 4: Overall accuracy and Kappa statistics of LULC maps of Diu Island using Confusion matrix

Parameters	**VEGETATION**	**AGRICULTURE**	**BUILT-UP**	**WATERBODY**	**OPEN LAND**	**TOTAL (USER)**	**User Accuracy**
Year:1991							
WILD VEGETATION	5	0	0	0	0	5	100%
ANTHROPOGENIC VEGETATION	0	5	0	0	0	5	100%
BUILT-UP	1	0	3	0	1	5	60%
WATERBODIES	0	0	0	5	0	5	100%
OPEN LAND	0	0	0	0	5s	5	100%
TOTAL (PRODUCER)	6	5	3	5	6	25	
Producer's Accuracy	83.33%	100%	100%	100%	83.33 %		
Overall Accuracy	92%						
Kappa Accuracy	90%						
Year: 2001							
WILD VEGETATION	5	0	0	0	0	5	100%
ANTHROPOGENIC VEGETATION	0	5	0	0	0	5	100%
BUILT-UP	0	0	5	0	0	5	100%
WATERBODIES	0	0	0	5	0	5	100%
OPEN LAND	0	1	0	0	4	5	80%
TOTAL (PRODUCER)	5	6	5	5	4	25	

Producer's Accuracy	100%	83.33	100%	100%	100%		
Overall Accuracy	96%						
Kappa Accuracy	95%						
Year: 2011							
WILD VEGETATION	5	0	0	0	0	5	100%
ANTHROPOGENIC VEGETATION	0	5	0	0	0	5	100%
BUILT-UP	0	0	5	0	0	5	100%
WATERBODIES	0	0	0	5	0	5	100%
OPEN LAND	0	1	0	0	4	5	80%
TOTAL (PRODUCER)	5	6	5	5	4	25	
Producer's Accuracy	100%	83.33	100%	100%	100%		
Overall Accuracy	96%						
Kappa Accuracy	95%						
Year: 2021							
WILD VEGETATION	4	1	0	0	0	5	80%
ANTHROPOGENIC VEGETATION	0	5	0	0	0	5	100%
BUILT-UP	0	0	5	0	0	5	100%
WATERBODIES	0	0	0	5	0	5	100%
OPEN LAND	0	0	0	0	5	5	100%
TOTAL (PRODUCER)	4	6	5	5	5	25	
Producer's Accuracy	100%	83.33%	100%	100%	100%		
Overall Accuracy	96%						
Kappa Accuracy	95%						

Table 5: Change detection in Diu city using post-classification comparison technique

CLASS	UNIT	1991	2001	2011	2021
WILD VEGETATION	Area (km^2)	-	1.32	2.76	0.74
	Change (%)	-	2.01	4.21	1.13
ANTHROPOGENIC VEGETATION	Area (km^2)	-	2.37	2.48	2.90
	Change (%)	-	3.62	3.79	4.42
BUILT-UP	Area (km^2)	-	1.40	1.12	2.33
	Change (%)	-	2.13	1.72	3.56
WATERBODIES	Area (km^2)	-	3.52	3.78	4.80
	Change (%)	-	5.37	5.76	7.32
OPEN LAND	Area (km^2)	-	14.57	12.01	7.19
	Change (%)	-	22.22	18.31	10.95

Table 6: Change in the area of each LULC class over 30 years (percentage).

Class	1991-2001 Area (%)	2001-2011 Area (%)	2011-2021 Area (%)
anthropogenic vegetation (No change)	3.62	3.79	4.42
Anthropogenic vegetation to built-up	0.74	0.31	3.99
anthropogenic vegetation to open land	1.48	0.64	0.48
anthropogenic vegetation to waterbody	1.72	0.64	1.54
Anthropogenic vegetation to wild vegetation	3.25	2.35	0.09
built-up (no change)	2.14	1.72	3.56
built-up to anthropogenic vegetation	1.39	0.95	0.32
built-up to open land	4.27	1.57	0.86
built-up to waterbody	0.61	0.74	1.00
Built-up to wild vegetation	0.33	0.37	0.00
open land (no change)	22.22	18.31	10.96
open land to anthropogenic vegetation	1.36	4.94	0.98
open land to built-up	2.06	3.38	5.94
open land to waterbody	0.91	2.18	5.07
open land to wild vegetation	0.18	0.55	0.03
waterbody (no change)	5.38	5.77	7.32
waterbody to anthropogenic vegetation	0.48	0.34	0.56
waterbody to built-up	0.29	0.27	1.16
waterbody to open land	1.20	1.73	0.89
Waterbody to wild	0.38	0.66	0.05

vegetation			
Wild Vegetation (No Change)	2.02	4.21	1.14
wild vegetation to anthropogenic vegetation	0.87	0.50	3.70
Wild vegetation to Built-up	0.13	0.07	0.24
wild vegetation to open land	0.19	0.72	0.10
wild vegetation to waterbody	0.15	0.65	2.97

Figure:1 Topographical Shape file of Diu Island prepared by using Google Earth

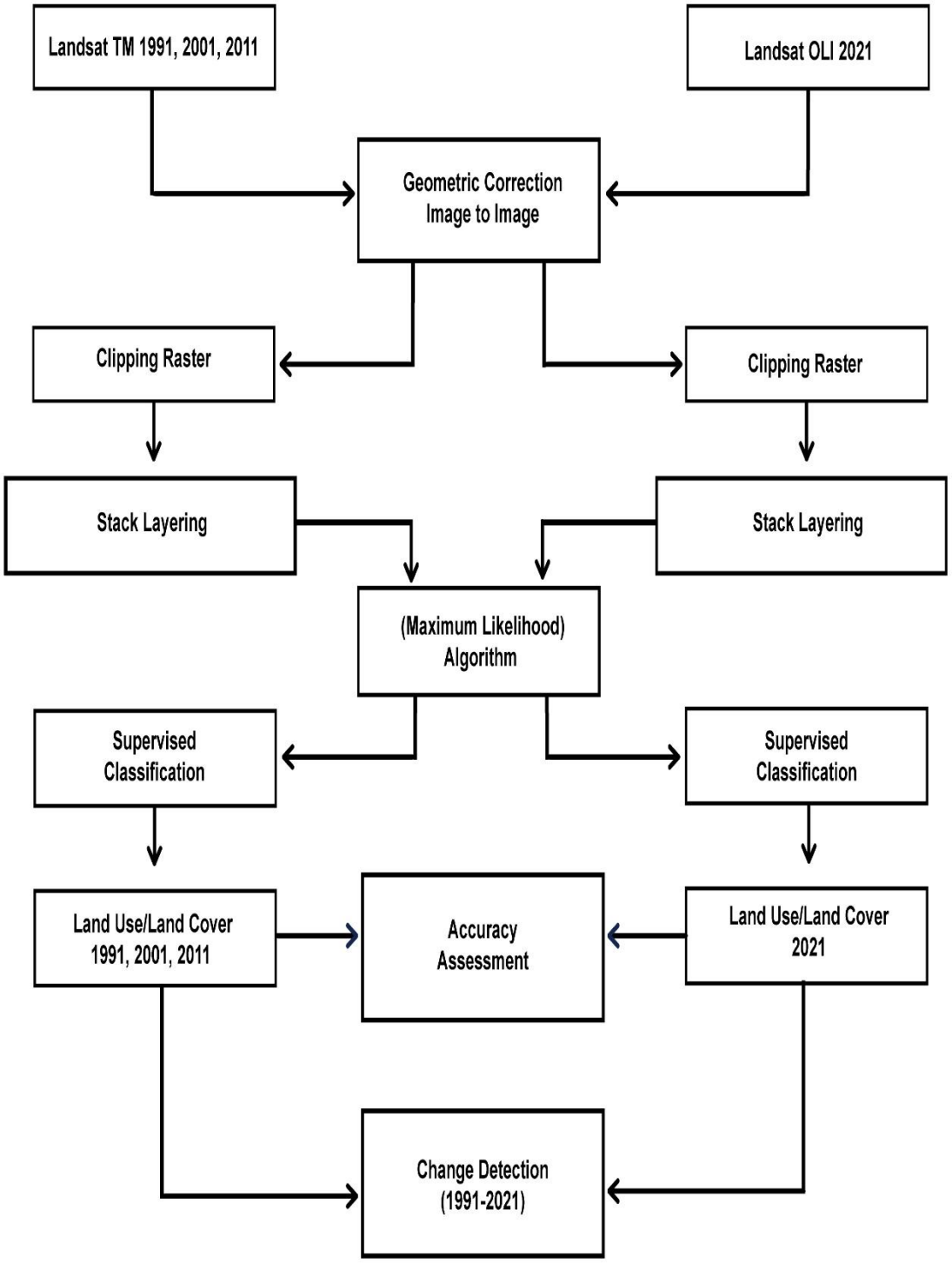

Figure:2 Flowchart of Methodology

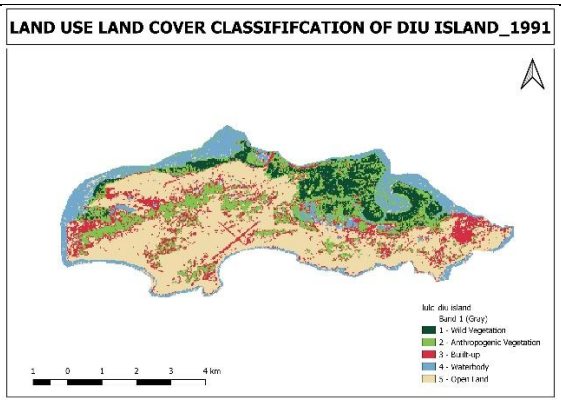

Year:1991

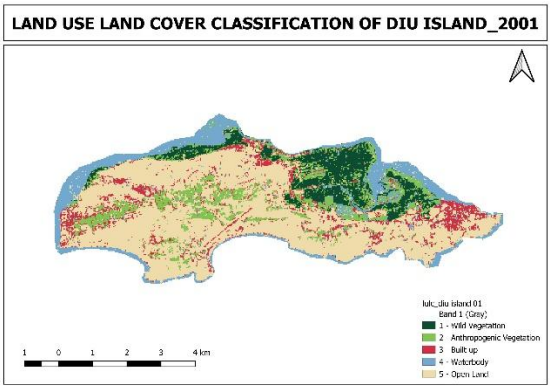

Year:2001

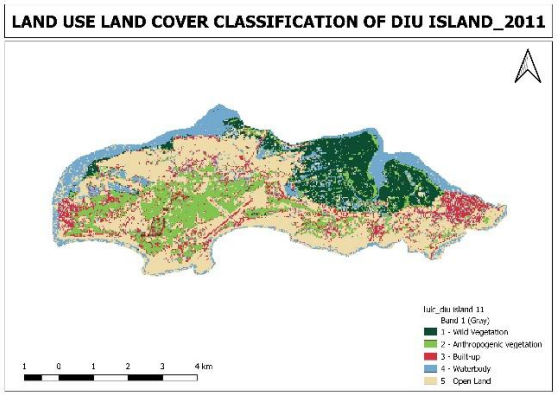

Year:2011

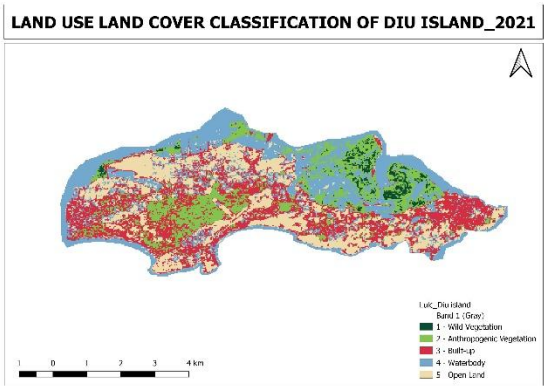

Year:2021

Figure:3 LULC Map of Diu Island

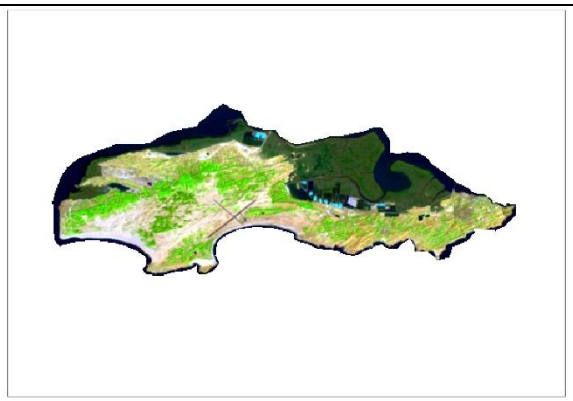	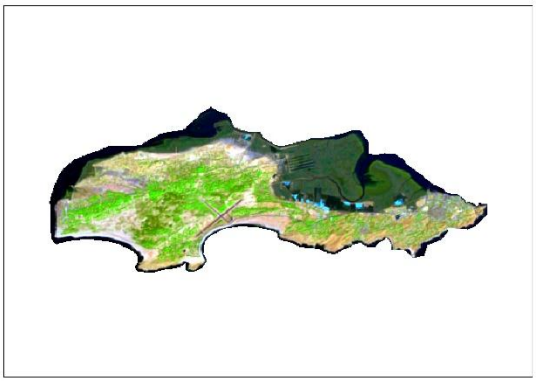
Year:1991	**Year:2001**
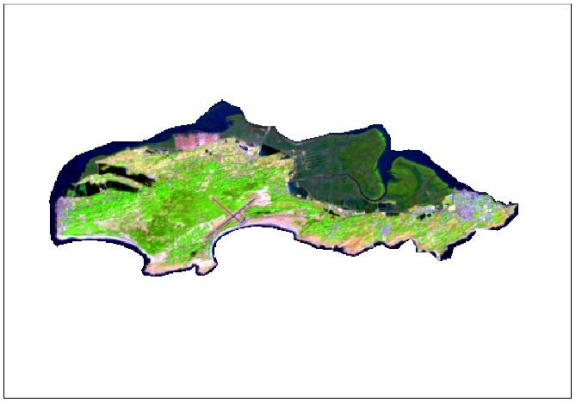	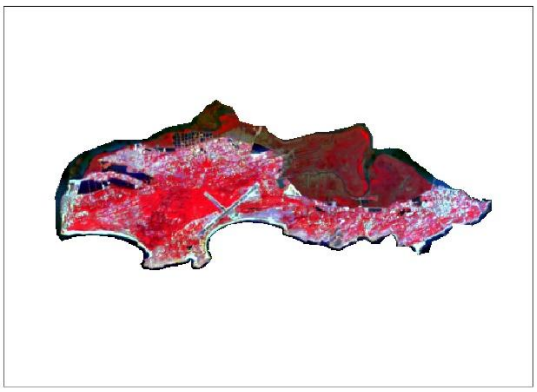
Year:2011	**Year:2021**

Figure:4 color infrared image (5-4-1) of the Diu Island prepared in QGIS 3.20.1

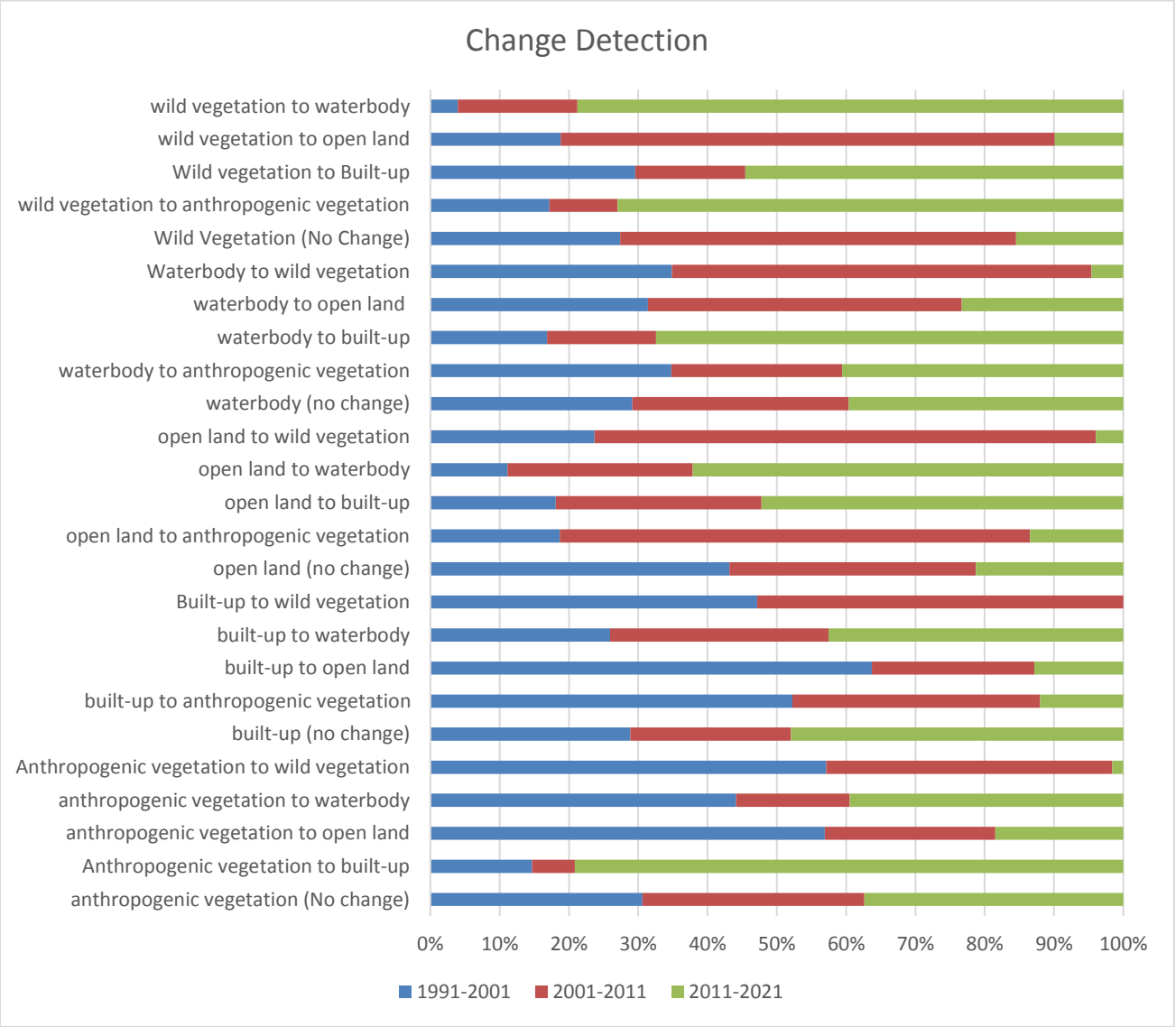

Figure: 5 Transition area of classes for the LULC from the year 1991 to 2021